

## A Motif-Based Network Analysis of Regulatory Patterns in Doxorubicin Effects on Treating Breast Cancer, a Systems Biology Study

Zeinab Dehghan<sup>1,2</sup>, Seyed Amir Mirmotalebisohi<sup>1,2</sup>, Marzieh Sameni<sup>1,2</sup>, Maryam Bazgiri<sup>3</sup>, and Hakimeh Zali<sup>4\*</sup>

1. Student Research Committee, Department of Medical Biotechnology, School of Advanced Technologies in Medicine, Shahid Beheshti University of Medical Sciences, Tehran, Iran

2. Cellular and Molecular Biology Research Center, Shahid Beheshti University of Medical Sciences, Tehran, Iran

3. Department of Animal Science, Agriculture and Natural Resources University of Khuzestan, Ahvaz, Iran

4. Department of Tissue Engineering and Applied Cell Sciences, School of Advanced Technologies in Medicine, Shahid Beheshti University of Medical Sciences, Tehran, Iran

### Abstract

**Background:** Breast cancer is the most common malignancy worldwide. Doxorubicin is an anthracycline used to treat breast cancer as the first treatment choice. Nevertheless, the molecular mechanisms underlying the response to Doxorubicin and its side effects are not comprehensively understood so far. We used systems biology and bioinformatics methods to identify essential genes and molecular mechanisms behind the body response to Doxorubicin and its side effects in breast cancer patients.

**Methods:** Omics data were extracted and analyzed to construct the protein-protein interaction and gene regulatory networks. Network analysis was performed to identify hubs, bottlenecks, clusters, and regulatory motifs to evaluate crucial genes and molecular mechanisms behind the body response to Doxorubicin and its side effects.

**Results:** Analyzing the constructed PPI and gene-TF-miRNA regulatory network showed that MCM3, MCM10, and TP53 are key hub-bottlenecks and seed proteins. Enrichment analysis also revealed cell cycle, TP53 signaling, Forkhead box O (FoxO) signaling, and viral carcinogenesis as essential pathways in response to this drug. Besides, SNARE interactions in vesicular transport and neurotrophin signaling were identified as pathways related to the side effects of Doxorubicin. The apoptosis induction, DNA repair, invasion inhibition, metastasis, and DNA replication are suggested as critical molecular mechanisms underlying Doxorubicin anti-cancer effect. SNARE interactions in vesicular transport and neurotrophin signaling and FoxO signaling pathways in glucose metabolism are probably the mechanisms responsible for side effects of Doxorubicin.

**Conclusion:** Following our model validation using the existing experimental data, we recommend our other newly predicted biomarkers and pathways as possible molecular mechanisms and side effects underlying the response to Doxorubicin in breast cancer requiring further investigations.

*Avicenna J Med Biotech 2022; 14(2): 137-153*

**Keywords:** Breast cancer, Doxorubicin, Protein-protein interaction network, Regulatory motif, Systems biology

### Introduction

Breast cancer is the most common cause of cancer and mortality caused by cancers in women worldwide<sup>1</sup>. Four subtypes of this cancer include luminal A and luminal B [expressing the Estrogen Receptor (ER)], basal-like, and Human Epidermal growth factor Receptor 2 (HER2)-enriched (without ER expression). This cancer is a heterogeneous disease at the molecular lev-

el. The characterization influence biologically-directed therapies and treatment de-escalation<sup>2</sup>. Breast cancer is often curable early, but the metastatic form is almost mortal due to therapeutic resistance<sup>3</sup>. The estrogen hormone and its receptor play essential roles in breast cancer progression. The dysregulation of the Estrogen Receptor (ER) is attributed to two-thirds of all breast

cancers. The ER receptor is one of the therapeutic targets for ER+ breast cancer<sup>4</sup>. In clinical diagnosis, 75% of breast tumors are ER+<sup>5</sup>; however, the role of ER signaling in metastasis of breast cancer remains poorly understood. Several studies have shown an adverse effect of ER signaling on motility and invasion of cells<sup>6,7</sup>, while a few studies suggested a positive effect of ER signaling on motility and invasion<sup>8,9</sup>.

Doxorubicin (DXR) is an anthracycline and chemotherapeutic drug isolated from *Streptomyces peuceitius*<sup>10</sup>. This drug is used to treat several cancers, including breast, gastric, lung, ovarian, thyroid, sarcoma, non-Hodgkins and Hodgkins lymphoma, multiple myeloma, and pediatric cancers<sup>11,12</sup>. DXR induces Reactive Oxygen Species release (ROS) that ROS lead to DNA damage, lipid peroxidation and membrane damage, and apoptotic cell death pathways<sup>13</sup>. DXR is among the chemotherapy drugs approved to treat ER+breast cancer. The response rates to DXR in patients exposed to DXR for the first time is reported to be 48%, and for more than once is 28%<sup>14</sup>. Nevertheless, little is known about the molecular basis of its effect on cell proliferation, estrogen/estrogen receptor signaling, and cell cycle progression<sup>15-17</sup>. Some investigations have even reported cardiotoxic side effects for DXR that their molecular mechanisms remain to be deciphered in detail<sup>18</sup>.

Systems biology and network-based methods are recently used to decipher the molecular mechanisms behind drugs and their possible side effects. Several such studies rely on network topology analysis to identify the effect of chemotherapy on various cancers. These networks can help understand how drugs influence the disease at the molecular level and identify the crucial gene sets underlying various drug effects<sup>19-22</sup>. Several network analysis studies of drug-disease associations have been used to predict drug side effects with high accuracy. Global expression data-based computational approaches can utilize gene interaction information for modeling Protein-Protein Interaction Networks (PPINs) and Gene Regulatory Networks (GRNs).

Identifying network modules and their biological functions helps decipher the molecular mechanisms of drug effects, identify new drug targets, predict body response to drugs, and organism behavior<sup>23-25</sup>. Gene regulatory networks contain information about regulatory elements of gene expression. These networks can identify regulatory programs and help understand the molecular basis of drug pharmacodynamics and even pharmacogenetics<sup>26</sup>. In 2020, a study analyzed the gene regulatory network of breast cancer and identified gene-specific personalized drug treatments<sup>27</sup>. Rao Zheng *et al* also constructed a gene regulatory network of diabetic nephropathy; they recognized essential genes using this method. These findings provide targets for drug development<sup>28</sup>. Adel Aloraini *et al*, in 2018, performed the identification of breast anti-cancer Docetaxel drug targets (DAXX and FGR1) using anal-

ysis of gene regulatory network and molecular docking<sup>29</sup>.

Molecular mechanisms mediating in breast cancer treatment by DXR and the mechanisms underlying its side effects are not still comprehensively understood. Therefore, in this study, we used protein-protein interaction and gene regulatory networks to identify essential molecular mechanisms and biological functions in response to DXR and the molecular mechanisms responsible for its side effects. We utilize a systems biology approach and bioinformatics analysis of protein-protein interaction network and Gene Regulatory Networks (GRNs) on omics data of breast cancer treatment using the DXR chemotherapeutic agents. Here, we utilize the protein-protein interaction modules and gene regulatory network motifs to predict and identify drug targets, Gene Ontology (GO) and biochemical pathways mediating in response to ER+ breast cancer and mechanisms underlying its side effects.

## Materials and Methods

### Data collection

Datasets on breast cancer (MCF-7 cell)/DXR were searched and collected from the *Gene Expression Omnibus (GEO)* database (<http://www.ncbi.nlm.nih.gov/geo/>) and proteomic publications<sup>30,31</sup>. Three datasets (GSE124597 (GPL 15207), GSE39870 (GPL 571), and GSE13477 (GPL 570)) were selected to compare breast cancer (MCF-7 cell line)/DXR and non-treatment breast cancer (MCF-7 cell line) for analysis in this study. Figure 1 shows the workflow of this study.

### Raw data processing and Data analysis

The datasets' Differentially Expressed Genes (DEGs) were analyzed and identified using GEO2R (<https://www.ncbi.nlm.nih.gov/geo/geo2r/>), which normalized the data using the GEO query and limma R package. The differentially expressed genes were iden-

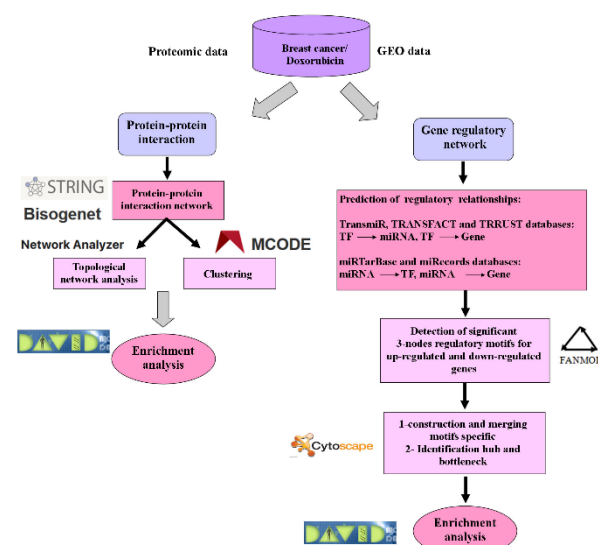


Figure 1. Study workflow.

tified according to  $p\text{-value} < 0.05$  and Fold Change cut-off of  $>0.5$  and  $<-0.5$  as a threshold. The genes obtained from the three datasets and proteomic publications (mass spectroscopy on MCF-7 treated compared to untreated) were used for further analysis.

#### **Protein-protein interaction network construction**

The shared DEGs between the three GSE datasets were obtained using the Venn diagram Tool<sup>32</sup> and unioned with DEGs data extracted from proteomic publications. We applied the STRING (Search Tool for the Retrieval of Interacting Genes/Proteins, <https://string-db.org>) with a confidence score of more than 0.7 and Bisogenet app [Human Protein Reference Database (HPRD)] to map the interactions of DEGs obtained from the shared nodes among the three GSE DEGs and unioned with proteomic publications. STRING is a biological database of known and predicted protein-protein interaction (physical and functional) for many organisms<sup>33</sup>. Bisogenet could build a relation between genes and their products in a fast and user-friendly manner and has multiple applications, including genomics information, protein-protein interactions, protein-DNA interactions, and gene ontology<sup>34</sup>. Bisogenet is available in Cytoscape software.

#### **Topological network analysis**

The PPI networks obtained from STRING and Bisogenet app were merged using Cytoscape software to analyze the interactions and connections between proteins (<http://www.cytoscape.org/>). Cytoscape software in bioinformatics for visualizing biomolecular interaction networks (protein-protein, protein-DNA, and genetics interactions) was available for humans and model organisms<sup>35</sup>.

This software contains several plugins for functional analysis in PPI networks. Cytoscape network analyzer is a tool that determines the degree and betweenness-centrality of every node as the hub and bottleneck genes. The hubs are node proteins with many interactions, and bottlenecks are nodes with high betweenness centrality<sup>35,36</sup>. Finding PPIN hubs and bottlenecks is used to candidate drug targets when drug designing. Besides, it is used to candidate possible disease markers<sup>37,38</sup>. We selected the top 10% of nodes with a higher degree and betweenness as hub-bottlenecks for further analysis.

#### **Molecular complex detection (MCODE) cluster sub-networks**

The STRING and Bisogenet PPI (HPRD database) networks were merged, and the resulted network was used to identify clusters using the MCODE Plug-in. The MCODE algorithm, one of the Cytoscape plugins, was used to identify highly interconnected sub-networks with parameter settings, including Degree Cutoff=2, Node Score Cutoff=0.2, K-Core=2, and Max-Depth=100<sup>39</sup>. We considered the MCODE score  $>3$  and the number of nodes  $>10$  as the final clusters' cut-off criteria.

#### **Functional enrichment analysis for hub-bottlenecks and MCODE clusters**

The enrichment analysis for Biological process, molecular function, and cellular component and KEGG biochemical pathways (Kyoto Encyclopedia of Genes and Genomes) were performed for the top 10% of the hub and bottleneck genes using the DAVID Tool (Database for Annotation, Visualization, and Integrated Discovery; <https://david.ncicrf.gov/>). DAVID is a bioinformatics resource for functional interpretation of a list of genes and can identify GO terms and visualize genes on the KEGG pathway<sup>40</sup>. The functional enrichment analysis was then performed for pathways of the sub-networks using the STRING database. For the enrichment analysis, STRING uses known systems such as Gene Ontology and KEGG<sup>41</sup>.

#### **TF-miRNA-gene regulatory networks Construction (for UP and down-regulated DEGs)**

The up and down-regulated DEGs among the three GSE datasets were identified separately using Venn diagram Tool<sup>32</sup>. The identified shared DEGs were unioned with up- and down-regulated proteins retrieved from proteomic publications results, separately. These up- and down-regulated genes were finally used to construct two separate regulatory networks for up- and down-regulated DEGs. The four relationships, including TF-gene, TF-miR, miR-gene, miR-TF, were extracted using the following tools and database to construct two gene regulatory networks for the gene sets.

#### **MiRNAs regulating DEGs**

The miRTarBase (<http://miRTarBase.mbc.nctu.edu.tw/>) and miRecords (<http://c1.accurascience.com/miRecords/>) databases were used for identifying miRNAs regulating genes and transcription factors. MiRecords is a database of experimentally validated miRNA-target interaction<sup>42</sup>. Besides, miRTarBase is a curated database of experimentally validated miRNA targets with high quality, and its miRNA-target interactions data are collected by receptor assay, microarray, next-generation sequencing, and western blot<sup>43</sup>.

#### **Transcription factors regulating DEGs**

The TFs regulating our target genes were extracted from the TRANSFAC (TRANSCRIPTION FACTOR; <https://genexplain.com/transfac/>) and TRRUST databases (transcriptional regulatory relationships unravelled by sentence-based text-mining; <https://www.grnpedia.org/trrust/>). TRANSFAC is a database of eukaryotic transcription factors and their experimentally-proven binding sites<sup>44</sup>. TRRUST is a curated database of human and mouse transcriptional regulatory networks, including 8444 TF-target interactions for 800 TFs in humans and 6552 regulatory interactions for 828 mouse TFs<sup>45</sup>.

#### **miRNAs inhibiting TFs**

The TFs regulating our target genes were fed into the miRTarBase and miRecords databases to obtain miRNAs targeting TFs.



### TFs regulating miRNAs

For identifying TFs regulating miRNAs, we used the TransmiR database (<http://www.cuilab.cn/transmir>). This database contains 3730 TF-miRNA regulations among 19 species from 1349 reports manually curated by surveying >8000 publications and more than 1.7 million tissue-specific TF-miRNA regulations incorporated based on ChIP-seq data <sup>46</sup>.

### Network construction, motif detection and motif specific sub-networks generation

In a gene regulatory network, network motifs are composed of nodes and regulations that connect the nodes. Some of these regulatory interaction patterns may be significantly high in some networks <sup>47</sup>. The molecular interactions of motifs are necessary to understand each motif's biological function <sup>48</sup>. To find the regulatory motifs in up-regulated and down-regulated gene networks, we used FANMOD software. The regulatory relationships (TF-miRNA, TF-Gene, miRNA-Gene, and miRNA-TF) were fed into the FANMOD to identify the motifs with three nodes. FANMOD is a tool for network motifs detection with detection motifs in a big network and analyzes colored networks <sup>49</sup>. This tool was used to build random networks 1000 times and compared it with the original input network. When randomizing the network in a constant global model, they indicate the frequency of motifs observed in the real network minus the mean of their occurrence in the random network divided by the standard deviation. The motifs with Z-score >2.0 and p-value <0.05 were selected as the significant motifs. TFs, genes and miRNAs participating in each motif were detected. The motif-related sub-networks of the up- and down-regulated DEGs were then merged (union) in Cytoscape software 3.5.1, separately. Finally, the top 10% of nodes with the highest degree (hub) and betweenness centrality (bottlenecks) were identified in the new networks, separately.

### Functional enrichment analysis of GRN

The up- and down-regulated DEGs of motif-related sub-networks were selected for functional enrichment analysis. The sets of DEGs participating in the union of the up- and down-regulated motif-related sub-networks were enriched by the DAVID Tool. The GO terms with p-value <0.05 were selected as significant.

## Results

### Raw data gathering and analysis

A total of 320 DEGs, including 126 up- and 194 down-regulated genes, were retrieved after analysing the datasets (GSE124597, GSE39870, and GSE1347) and collecting proteomics publications data. Supplementary figure 1 shows the resulted Venn diagram. Supplementary table S1 represents all the up- and down-regulated DEGs

### Construction of PPI network

The PPI network was constructed for DEGs using STRING and Bisogenet app (HPRD database) for map-

ping interactions and then merging. The resulted network consisted of 320 nodes and 2519 edges.

### Topological analysis

The network analyzer tool was used to study the topological network properties and identify the crucial hub and bottleneck nodes. The topological network properties included the clustering coefficient of 0.385, the shortest path of 60362, network density of 0.045, and diameter of 7. Figure 2 represents a sub-network including the 10% of the genes with the highest degree and betweenness centrality as hubs and bottlenecks, respectively. The top ten hubs and bottlenecks are listed in table 1. The list of 10% of the genes with the highest degree and betweenness centrality are reported in Supplementary table S2.

### Module detection

Further analysis of complexes by MCODE app in Cytoscape software revealed 13 sub-networks. The PPI sub-networks are highly connected regions of the network. Three sub-networks were selected according to score >3 and nodes >10 (Table 2, Figure 3). The seed-

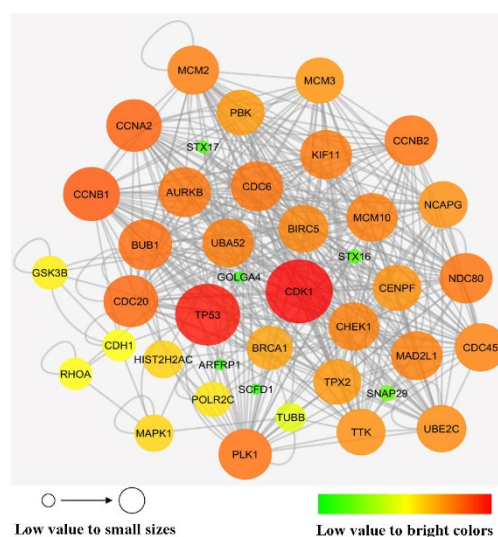


Figure 2. Protein-protein interaction network. The sub-network constructed by Cytoscape software encompasses 10% of hubs and bottlenecks. The nodes' size and color are based on their degree value, and Nodes with dark color (red) have the highest degree.

Table 1. Hub genes related to the breast cancer-doxorubicin network obtained from Cytoscape software

| Name genes   | Degree | Betweenness centrality |
|--------------|--------|------------------------|
| <i>CDK1</i>  | 111    | 0.06099772             |
| <i>TP53</i>  | 105    | 0.29304896             |
| <i>CCNB1</i> | 82     | 0.03575425             |
| <i>CCNA2</i> | 78     | 0.01470353             |
| <i>CDC20</i> | 76     | 0.01682273             |
| <i>BUB1</i>  | 73     | 0.0130227              |
| <i>PLK1</i>  | 72     | 0.02161398             |
| <i>CCNB2</i> | 71     | 0.00729474             |
| <i>NDC80</i> | 71     | 0.00428032             |
| <i>CDC6</i>  | 70     | 0.014245               |

Table 2. The PPI sub-networks with Score&gt;3 and nodes&gt;10

| Sub-networks | Score  | Density nodes | Number of Interactions | Seed node |
|--------------|--------|---------------|------------------------|-----------|
| 1            | 40.227 | 45            | 916                    | MCM10     |
| 2            | 7      | 15            | 52                     | MCM3      |
| 3            | 4.941  | 18            | 43                     | NAPRT     |

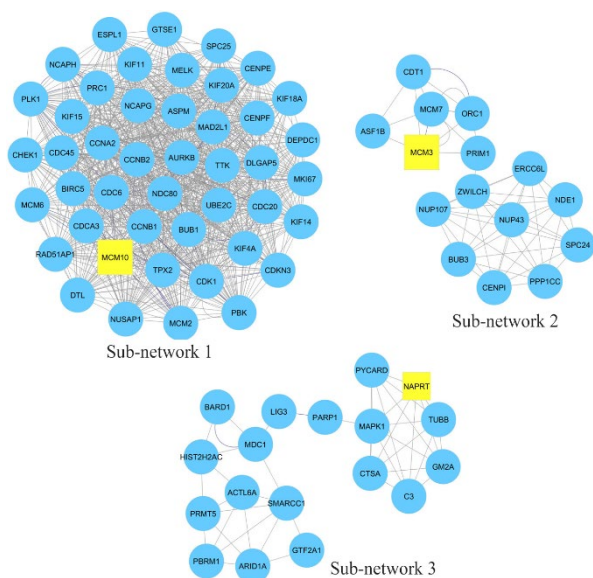


Figure 3. The PPI sub-networks based on highly connected-regions. Sub-networks 1, 2, and 3 were selected based on Score>3 and nodes> 10. Yellow rectangles represent seed nodes.

nodes of these sub-networks included MCM10 (Minichromosome Maintenance 10 Replication Initiation Factor) for sub-network No.1, MCM3 (Minichromosome Maintenance 3 Replication Initiation Factor) for sub-network No.2, and NAPRT (Nicotinate Phosphoribosyltransferase) for sub-network No.3. The results are depicted in table 3. The nodes related to sub-networks are shown in Supplementary table S3.

#### Gene ontology and KEGG pathway enrichment

We performed Gene Ontology analyses for 10% of hubs and bottleneck genes using the DAVID database.

Table 4 shows the resulting gene ontology terms. Biological process terms reveal that most of the hub genes participate in regulating the cell cycle. The top 10 related molecular functions identified using the DAVID database mediated in protein binding, nucleic acid-binding, etc. The cellular component terms showed that most hub genes were present in the cytoskeleton, chromosomes, etc.

The DAVID database's KEGG pathway analysis demonstrated that hub and bottleneck genes were involved in the cell cycle, Tumor protein 53 (Tp53) signaling pathway, viral carcinogenesis, viral infections, Forkhead box O (FoxO) signaling pathway, and adherent junctions. Besides, the KEGG pathway analysis showed that SNARE interactions in vesicular transport and neurotrophin signaling pathway were of a significant p-value in enrichment. They could be hypothesized and studied as a signaling possibly related to some side effects of DXR. Table 4 contains the top results of the KEGG pathway analysis by the DAVID database. Supplementary table S4 contains all gene ontology and pathways data related to 10% hub and bottleneck genes.

The top pathway terms significantly enriched in sub-network No.1 included the cell cycle, p53 signaling pathway, viral carcinogenesis, FoxO signaling pathway, and DNA replication. Biochemical pathways involved in sub-network No.2 included cell cycle and DNA replication. The nodes in sub-network No.3 were related to viral carcinogenesis (Table 3).

#### TF-miRNA-gene regulatory network construction

**Identification of miRNA-gene/TF and TF-miRNA/gene interactions:** In this study, miRNAs regulating post-transcriptional mRNAs were retrieved from the two experimentally validated databases, including miRTarBase and miRecords. The up-regulated genes obtained from three GSE and proteomics data were targeted with 1082 miRNAs through 2103 interaction, and the transcription factors regulating genes were identified using TRANSFAC and TRRUST databases. The results revealed that 227 TFs regulated the target genes through 1088 interactions. The number of 1444 miRNAs targeted 152 TFs with 5979 interactions. TFs regulating miRNAs identified by the validated data of the

Table 3. KEGG pathway analysis of sub-networks

| KEGG ID              | Terms                  | p-value     | Genes  |
|----------------------|------------------------|-------------|--|
| <b>Sub-network 1</b> |                        |             |  |
| hsa04110             | Cell cycle             | 1.17E-22    | <i>PLK1, TTK, CDC6, CCNA2, CDC20, CCNB2, ...</i> |
| hsa04115             | p53 signaling pathway  | 1.78E-05    | <i>CCNB2, CCNB1, CHEK1, CDK1, GTSE1</i>          |
| hsa05203             | Viral carcinogenesis   | 0.013025793 | <i>CCNA2, CDC20, CHEK1, CDK1</i>                 |
| hsa04068             | FoxO signaling pathway | 0.042317087 | <i>CCNB2, CCNB1, PLK1</i>                        |
| <b>Sub-network 2</b> |                        |             |  |
| hsa04110             | Cell cycle             | 1.90E-04    | <i>MCM7, ORC1, MCM3, BUB3</i>                    |
| hsa03030             | DNA replication        | 5.50E-04    | <i>MCM7, PRIMI, MCM3</i>                         |
| <b>Sub-network 3</b> |                        |             |  |
| hsa05203             | Viral carcinogenesis   | 0.040723    | <i>C3, GTF2A1, MAPK1</i>                         |

## Regulatory Motifs in Doxorubicin Effects

Table 4. Top 10 biological processes, molecular functions, cellular components, and KEGG pathways of 10% hub and bottleneck genes identified using the DAVID database (sorted based on p-value <0.05)

| ID                        | Terms  | p-value     | Genes   |
|---------------------------|--|-------------|---|
| <b>Biological process</b> |  |             |   |
| GO:1903047                | mitotic cell cycle process                   | 5.11E-26    | <i>NCAPG, MCM10, TTK, KIF11, AURKB, CDC20, CCNB2, ...</i> |
| GO:0000278                | mitotic cell cycle                           | 4.81E-25    | <i>NCAPG, MCM10, TTK, KIF11, AURKB, CDC20, CCNB2, ...</i> |
| GO:0022402                | Cell cycle process                           | 4.38E-24    | <i>GSK3B, NCAPG, MCM10, TTK, BRCA1, KIF11, ...</i>        |
| GO:0044772                | mitotic cell cycle phase transition          | 9.66E-24    | <i>UBE2C, TUBB, PLK1, TTK, MCM10, CDC6, NDC80, ...</i>    |
| GO:0044770                | Cell cycle phase transition                  | 3.77E-23    | <i>UBE2C, TUBB, PLK1, TTK, MCM10, CDC6, NDC80, ...</i>    |
| GO:0007049                | Cell cycle                                   | 5.82E-23    | <i>GSK3B, NCAPG, MCM10, TTK, BRCA1, KIF11, ...</i>        |
| GO:0007067                | mitotic nuclear division                     | 4.28E-22    | <i>UBE2C, PLK1, NCAPG, TTK, KIF11, CDC6, RHOA, ...</i>    |
| GO:0010564                | Regulation of cell cycle process             | 8.14E-21    | <i>UBE2C, PLK1, TTK, BRCA1, KIF11, CDC6, RHOA, ...</i>    |
| GO:0000075                | Cell cycle checkpoint                        | 2.37E-20    | <i>PLK1, TTK, BRCA1, CDC6, NDC80, AURKB, CCNA2, ...</i>   |
| GO:0000280                | Nuclear division                             | 1.70E-19    | <i>UBE2C, PLK1, NCAPG, TTK, KIF11, CDC6, RHOA, ...</i>    |
| <b>Molecular function</b> |  |             |   |
| GO:0005515                | Protein binding                              | 2.71E-08    | <i>GSK3B, STX17, STX16, NCAPG, MCM10, TTK, BRCA1, ...</i> |
| GO:0035639                | Purine ribonucleoside triphosphate binding   | 2.87E-08    | <i>GSK3B, UBE2C, TUBB, PLK1, TTK, KIF11, CDC6, ...</i>    |
| GO:0032550                | Purine ribonucleoside binding                | 3.10E-08    | <i>GSK3B, UBE2C, TUBB, PLK1, TTK, KIF11, CDC6, ...</i>    |
| GO:0032549                | Ribonucleoside binding                       | 3.18E-08    | <i>GSK3B, UBE2C, TUBB, PLK1, TTK, KIF11, CDC6, ...</i>    |
| GO:0001883                | Purine nucleoside binding                    | 3.18E-08    | <i>GSK3B, UBE2C, TUBB, PLK1, TTK, KIF11, CDC6, ...</i>    |
| GO:0001882                | Nucleoside binding                           | 3.37E-08    | <i>GSK3B, UBE2C, TUBB, PLK1, TTK, KIF11, CDC6, ...</i>    |
| GO:0032555                | Purine ribonucleotide binding                | 4.12E-08    | <i>GSK3B, UBE2C, TUBB, PLK1, TTK, KIF11, CDC6, ...</i>    |
| GO:0017076                | Purine nucleotide binding                    | 4.59E-08    | <i>GSK3B, UBE2C, TUBB, PLK1, TTK, KIF11, CDC6, ...</i>    |
| GO:0032553                | Ribonucleotide binding                       | 4.70E-08    | <i>GSK3B, UBE2C, TUBB, PLK1, TTK, KIF11, CDC6, ...</i>    |
| GO:0004674                | Protein serine/threonine kinase activity     | 5.55E-08    | <i>GSK3B, CCNB2, CCNB1, PLK1, CHEK1, PBK, CDK1, ...</i>   |
| <b>Cellular component</b> |  |             |   |
| GO:0015630                | microtubule cytoskeleton                     | 1.04E-18    | <i>GSK3B, TUBB, PLK1, NCAPG, TTK, BRCA1, KIF11, ...</i>   |
| GO:0005856                | Cytoskeleton                                 | 5.37E-15    | <i>GSK3B, NCAPG, TTK, BRCA1, KIF11, AURKB, CDC20, ...</i> |
| GO:0044427                | Chromosomal part                             | 1.42E-14    | <i>PLK1, NCAPG, TTK, MCM10, BRCA1, NDC80, AURKB, ...</i>  |
| GO:0044430                | Cytoskeletal part                            | 2.93E-14    | <i>GSK3B, TUBB, PLK1, NCAPG, TTK, BRCA1, KIF11, ...</i>   |
| GO:0043228                | Non-membrane-bounded organelle               | 3.89E-14    | <i>GSK3B, NCAPG, MCM10, TTK, BRCA1, KIF11, ...</i>        |
| GO:0043232                | Intracellular non-membrane-bounded organelle | 3.89E-14    | <i>GSK3B, NCAPG, MCM10, TTK, BRCA1, KIF11, ...</i>        |
| GO:0005694                | Chromosome                                   | 1.20E-13    | <i>PLK1, NCAPG, TTK, MCM10, BRCA1, NDC80, AURKB, ...</i>  |
| GO:0005819                | Spindle                                      | 9.41E-13    | <i>PLK1, TTK, KIF11, CDC6, AURKB, CDC20, TPX2, ...</i>    |
| GO:0044446                | Intracellular organelle part                 | 1.61E-12    | <i>GSK3B, STX17, STX16, NCAPG, MCM10, TTK, BRCA1, ...</i> |
| GO:0005815                | microtubule-organizing center                | 1.74E-12    | <i>GSK3B, PLK1, NCAPG, BRCA1, AURKB, CDC20, ...</i>       |
| <b>KEGG</b>               |  |             |   |
| hsa04110                  | Cell cycle                                   | 8.81E-20    | <i>GSK3B, PLK1, TTK, CDC6, CCNA2, CDC20, CCNB2, ...</i>   |
| hsa04115                  | p53 signaling pathway                        | 1.41E-04    | <i>CCNB2, CCNB1, CHEK1, CDK1, TP53</i>                    |
| hsa05203                  | Viral carcinogenesis                         | 1.42E-04    | <i>CCNA2, CDC20, CHEK1, CDK1, MAPK1, TP53, RHOA</i>       |
| hsa04130                  | SNARE interactions in vesicular transport    | 0.008270639 | <i>STX17, STX16, SNAP29</i>                               |
| hsa04722                  | Neurotrophin signaling pathway               | 0.012342719 | <i>GSK3B, MAPK1, TP53, RHOA</i>                           |
| hsa04068                  | FoxO signaling pathway                       | 0.016591619 | <i>CCNB2, CCNB1, PLK1, MAPK1</i>                          |
| hsa05130                  | Pathogenic Escherichia coli infection        | 0.018014118 | <i>CDH1, TUBB, RHOA</i>                                   |
| hsa05166                  | HTLV-I infection                             | 0.018496934 | <i>CDC20, GSK3B, CHEK1, TP53, MAD2L1</i>                  |
| hsa04520                  | Adherens junction                            | 0.033403027 | <i>CDH1, MAPK1, RHOA</i>                                  |
| hsa04110                  | Cell cycle                                   | 8.81E-20    | <i>GSK3B, PLK1, TTK, CDC6, CCNA2, CDC20, CCNB2, ...</i>   |

TransmiR database revealed 356 TFs regulated 323 miRNAs with 2011 interactions.

The 194 down-regulated genes obtained from the three GSE datasets and proteomics data were regulated by 1027 miRNAs and 209 TFs through 2457 and 1458 interactions. The number of 1451 miRNAs targeted 133 TFs with 5862 interactions. The analysis of TFs regulating miRNAs by TransmiR revealed that 354

TFs regulated 320 miRNAs with 2008 interactions obtained from experimentally validated data. Finally, the miRNA-gene, TF-Gene, miR-TF, and TF-miR interactions were incorporated to construct two regulatory networks in Cytoscape. The results are shown in table 5. Supplementary table S5 and table S6 contain all relationships in up-regulated and down-regulated, respectively.



Table 5. Summary of four types of regulatory relationships among miRNA-gene, TF-Gene, miR-TF, and TF-miR interactions

| Relationship          | Number of pairs | Number of genes | Number of TFs | Number of miRNAs |
|-----------------------|-----------------|-----------------|---------------|------------------|
| <b>Up-regulated</b>   |                 |                 |               |                  |
| miRNA-gene            | 2103            | 52              | -             | 1082             |
| miR-TF                | 5979            | -               | 152           | 1445             |
| TF-Gene               | 1088            | 56              | 227           | -                |
| TF-miR                | 2011            | -               | 356           | 323              |
| <b>Down-regulated</b> |                 |                 |               |                  |
| miRNA-gene            | 2457            | 88              | -             | 1027             |
| miR-TF                | 5862            | -               | 133           | 1451             |
| TF-Gene               | 1558            | 87              | 209           | -                |
| TF-miR                | 2008            | -               | 354           | 320              |

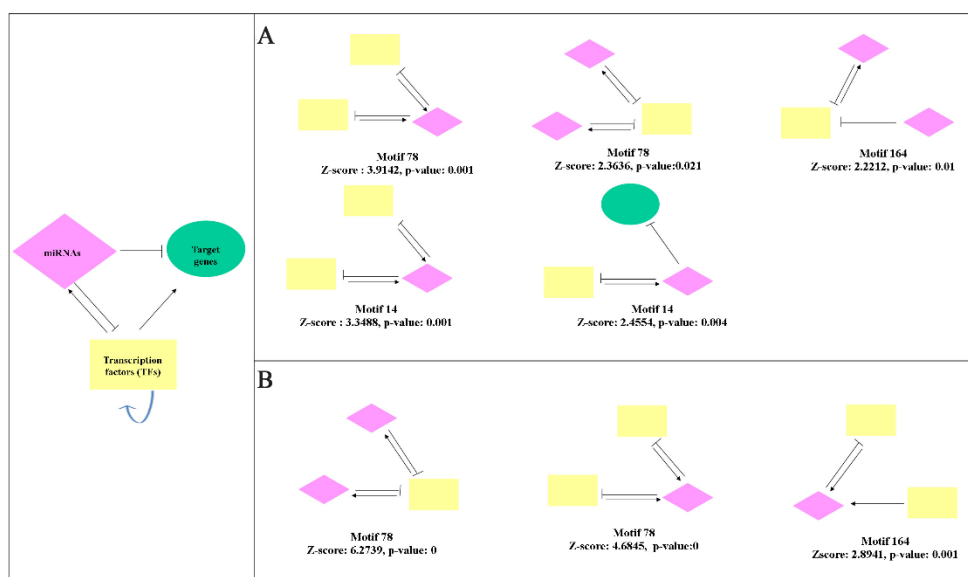


Figure 4. Regulatory motifs consist of miRNAs, TFs, and target genes detected in up and down-regulated gene networks with their Z-score and their p-value. Three types of relationships involved in these motifs included miRNA-gene (miRNA represses gene expression); miRNA-TF (miRNA represses TF gene expression); and TF-miRNA (TF regulates miRNA expression).

#### Motif detection and generating motif-specific sub-networks

The miRNA-gene, TF-Gene, miRNA-TF, TF-miRNA relationships were combined, and the regulatory networks were constructed. The up- and down-regulated gene networks contained 2250 and 2251 nodes, respectively. The FANMOD software was used to detect the motifs. The types of identified motifs are represented in figure 4 for up- and down-regulated gene networks.

We selected motifs with  $Z\text{-score} > 2$ ,  $p\text{-value} < 0.05$ , and at least two-color edges (two types of interactions). Motifs with identification numbers 14, 78, and 164 were finally selected in the up-regulated network. The sub-networks related to these motifs were merged to create a network, including 64 miRNAs, 53 genes, and 321 TFs. The regulatory sub-networks were visualized by Cytoscape 3.5.1. (Figure 5A). Motifs No.78 and 164 were selected and merged in the down-regulated network to create a sub-network including 77 miRNAs, eight genes, and 274 TFs (Figure 5B).

The topological analysis of up and down-regulated GRNs identified the BTG Anti-Proliferation Factor 2

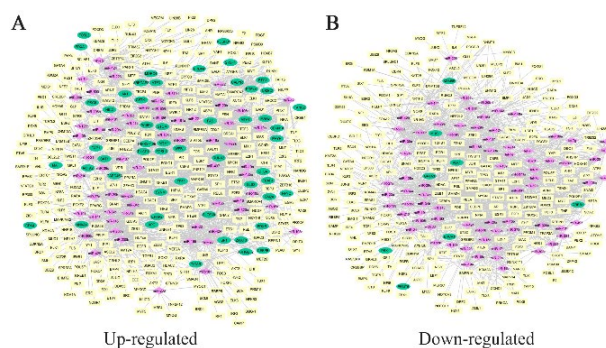


Figure 5. Regulatory sub-networks. A) The sub-network was generated by merging motifs No.14, 78, and 164 in the up-regulated gene network. B) Merging motifs No.78 and 164 in the down-regulated network. Pink diamond nodes are miRNAs, green circular show genes, and yellow rectangles represent the transcription factors.

(BTG2), Specificity Protein 1 (SP1), and TP53 as hub-bottleneck, which were also present in up-regulated sub-network. However, none of the genes in the down-regulated sub-network was among the GRN 10% of hub-bottlenecks.

#### Gene ontology and biochemical pathway enrichment analysis

For Gene Ontology analysis, genes obtained from motif detection were submitted in the DAVID database. The top 10 Biological process terms included regulation of cell death and the metabolic process, nucleic acid-binding, transcription binding are top 10 in molecular function terms. The cellular components showed the nucleus and organelle as the top related to the gene-set. The significant pathways were identified from analysis of genes in motif-related sub-networks using the DAVID database. The significant pathways included the p53 signaling pathway, transcriptional misregulation in cancer, cell cycle, PI3K-Akt signaling pathway, viral carcinogenesis, viral infection, Measles, and FoxO signaling pathway (Table 6). Supplementary table S7 contains all gene ontology and KEGG pathways data related to the gene set.

#### Discussion

Breast cancer is the most common malignancy in women. Its molecular heterogeneity influences the selection of methods in the effective treatment of this cancer<sup>2</sup>. Treatment of routine surgery, radiation therapy, chemotherapy, stabilizing agents, enzyme inhibitors, and immunotherapy are used to treat breast cancer. DXR is an effective chemotherapeutic drug of the anthracycline family used to treat breast cancer<sup>50</sup>. A comprehensive understanding of the molecular mechanisms of DXR in the treatment of breast cancer is still lacking<sup>51</sup>. The systems biology approach and bioinformatical network analysis for breast cancer in response to DXR help candidate essential genes and pathways mediating in response to this drug for further experimental examinations. The identified and validated targets and pathways may even be used to repurpose new drugs.

Network-based approaches have recently appeared to be a powerful tool to investigate pathobiological processes and the molecular complexity of disease aetiology by identifying disease-specific network clusters such as MCODE clusters in PPI networks. The nodes participating in these particular regions usually have critical roles and biological functions<sup>52</sup>. Nodes participating in regulatory motifs also are of biological importance in GRNs<sup>53</sup>. We applied the MCODE clusters and GRN motifs to predict the molecular mechanisms underlying the treating effect of DXR on breast cancer and its side effects. This study selected genomics and proteomics data to integrate and explore critical genes and molecular pathways. The present study is the first *in silico* analysis that uses bioinformatics analysis to

predict the essential genes and pathways of breast cancer treated with DXR and its side effects.

Our systematic analysis of the PPI MCODE clusters and GRN motif-related sub-networks of the MCF7 cell line in response to DXR demonstrated that TP53, MCM10, and MCM3 are the top hub-bottlenecks and MCODE cluster seeds in response to DXR (Supplementary table S8). The functional enrichment analysis indicated that hub-bottleneck and cluster nodes were involved in the cell cycle, P53 signaling pathway, FoxO signaling pathway, and viral carcinogenesis.

TP53 is a hub-bottleneck protein in our PPIN and GRN. TP53 is a gene with a high degree and betweenness centrality over-expressed in the MCF-7 cell line in response to DXR. This protein can recognize DNA damage, stop the cell cycle at the G1/S regulation point, and activate DNA repair proteins. Therefore, TP53 can initiate apoptosis if DNA damage is irreparable<sup>54</sup>. TP53 was up-regulated in MCF-7 cells treated with DXR. Therefore, it can be concluded that DXR activates the repair system and instigates apoptosis in cancer cells possible through P53 mediation.

The Minichromosome Maintenance proteins (MCM) are critical regulators in DNA replication<sup>55</sup>. These proteins are implicated in cancer initiation and progression, and their expression is up-regulated in a wide range of epithelial malignancies<sup>56</sup>. MCM10, an MCM family member, is an essential factor for DNA replication by binding with Cell Division Cycle 45 (CDC45) and is essential in breast cancer progression<sup>57</sup>. Alcivar *AL et al* reported that cells depleted of MCM10 showed instability of replication fork<sup>58</sup>. Wei-Dong Yang *et al* in 2019 showed MCM10 was significantly over-expressed in breast carcinoma and involved in proliferation, migration, and invasion. Therefore, it can induce metastasis *via* the Wnt/ $\beta$ -catenin pathway in breast cancer<sup>59</sup>. Our results identified MCM10 as a critical node in the network. Given the importance of this protein and the lack of experimental literature about its mediation in response to DXR, we suggest that its experimental investigation seems necessary.

MCM3, another MCM member, is over-expressed in various human cancers<sup>60</sup>. MCM3 is one of the cell cycle markers that regulates the growth, migration, and invasion of cells<sup>61</sup>. Our study showed that MCM3 was also a down-regulated protein of importance in the networks. Therefore, we hypothesize that DXR can probably inhibit DNA replication, invasion, and metastasis by down-regulating the *MCM10* and *MCM3* genes.

The functional enrichment analysis showed regulation of the cell cycle, p53 signaling, viral carcinogenesis, Human T-Lymphotropic Virus type 1 (HTLV-1) infection, and FoxO signaling pathway were the top terms related to hubs and bottlenecks in PPIN, MCODE clusters, and GRNs. Besides, Soluble N-ethylmaleimide-sensitive factor Attachment protein



Table 6. The table represents the top 10 biological processes, molecular function, cellular components, and KEGG pathways identified using the DAVID tool (sorted based on p-value&lt;0.05)

| GO ID                     | Terms   | p-value  | Genes   |
|---------------------------|---|----------|---|
| <b>Biological process</b> |   |          |   |
| GO:0010941                | Regulation of cell death  | 4.37E-10 | <i>CDKN1A, TIGAR, BTG2, CEBPB, GADD45A, ...</i>         |
| GO:0010604                | Positive regulation of macromolecule metabolic process  | 4.69E-10 | <i>FOXAI, KDM5B, CDKN1A, BTG2, CEBPB, ...</i>           |
| GO:0042981                | Regulation of the apoptotic process   | 6.86E-10 | <i>CDKN1A, TIGAR, BTG2, CEBPB, GADD45A, ...</i>         |
| GO:0043067                | Regulation of programmed cell death   | 8.18E-10 | <i>CDKN1A, TIGAR, BTG2, CEBPB, GADD45A, ...</i>         |
| GO:0008219                | Cell death  | 2.29E-09 | <i>CDKN1A, BTG2, CEBPB, GLS2, GATA3, ...</i>            |
| GO:0009893                | Positive regulation of the metabolic process  | 2.54E-09 | <i>FOXAI, KDM5B, CDKN1A, BTG2, CEBPB, ...</i>           |
| GO:0031325                | Positive regulation of cellular metabolic process   | 1.09E-08 | <i>FOXAI, CDKN1A, BTG2, CEBPB, SRSF1, ...</i>           |
| GO:0012501                | Programmed cell death   | 2.31E-08 | <i>CDKN1A, TIGAR, BTG2, CEBPB, GADD45A, ...</i>         |
| GO:0010628                | Positive regulation of gene expression  | 2.33E-08 | <i>FOXAI, KDM5B, CEBPB, NFYC, SRSF1, ...</i>            |
| GO:0006915                | Apoptotic process   | 4.17E-08 | <i>CDKN1A, TIGAR, BTG2, CEBPB, GADD45A, ...</i>         |
| <b>Molecular function</b> |   |          |   |
| GO:0000982                | Transcription factor activity, RNA polymerase II core promoter proximal region sequence-specific binding        | 1.27E-09 | <i>FOXAI, BTG2, CEBPB, NFYC, GATA3, ...</i>             |
| GO:0044212                | Transcription regulatory region DNA binding   | 1.61E-09 | <i>FOXAI, PRMT5, CEBPB, GADD45A, NFYC, ...</i>          |
| GO:0000975                | Regulatory region DNA binding   | 1.70E-09 | <i>FOXAI, PRMT5, CEBPB, GADD45A, NFYC, ...</i>          |
| GO:0001067                | Regulatory region nucleic acid binding  | 1.73E-09 | <i>FOXAI, PRMT5, CEBPB, GADD45A, NFYC, ...</i>          |
| GO:0001228                | Transcriptional activator activity, RNA polymerase II transcription regulatory region sequence-specific binding | 9.84E-09 | <i>FOXAI, FOSL1, CEBPB, CREB1, MAF, MAFB, ...</i>       |
| GO:0000981                | RNA polymerase II transcription factor activity, sequence-specific DNA binding                                  | 2.86E-08 | <i>FOXAI, BTG2, CEBPB, NFYC, GATA3, ...</i>             |
| GO:0000987                | Core promoter proximal region sequence-specific DNA binding   | 4.26E-08 | <i>FOSL1, MUC1, CEBPB, CREB1, MAFB, SPI, ...</i>        |
| GO:0003690                | Double-stranded DNA binding   | 4.45E-08 | <i>PRMT5, CEBPB, NFYC, XPC, GATA3, RUNX2, ...</i>       |
| GO:0001159                | Core promoter proximal region DNA binding   | 4.50E-08 | <i>FOSL1, MUC1, CEBPB, CREB1, MAFB, SPI, ...</i>        |
| GO:0000976                | Transcription regulatory region sequence-specific DNA binding   | 4.98E-08 | <i>PRMT5, CEBPB, NFYC, GATA3, RUNX2, ...</i>            |
| <b>Cellular component</b> |   |          |   |
| GO:0070013                | Intracellular organelle lumen   | 1.61E-06 | <i>FOXAI, KDM5B, CDKN1A, CEBPB, GLS2, ...</i>           |
| GO:0043233                | Organelle lumen   | 2.34E-06 | <i>FOXAI, KDM5B, CDKN1A, CEBPB, GLS2, ...</i>           |
| GO:0031974                | Membrane-enclosed lumen   | 3.13E-06 | <i>FOXAI, KDM5B, CDKN1A, CEBPB, GLS2, ...</i>           |
| GO:0005667                | Transcription factor complex  | 7.01E-06 | <i>CEBPB, CREB1, MAFB, CDK4, NFYC, GATA3, ...</i>       |
| GO:0031981                | Nuclear lumen   | 1.77E-05 | <i>FOXAI, KDM5B, CDKN1A, CEBPB, SRSF1, ...</i>          |
| GO:0000785                | Chromatin   | 1.93E-05 | <i>MUC1, CEBPB, CREB1, MAF, SPI, CDK4, ...</i>          |
| GO:0005654                | Nucleoplasm   | 2.81E-05 | <i>CTSA, KDM5B, PRMT5, CDKN1A, CEBPB, ...</i>           |
| GO:0044428                | Nuclear part  | 3.71E-05 | <i>FOXAI, KDM5B, CDKN1A, CEBPB, SRSF1, ...</i>          |
| GO:0005634                | Nucleus   | 5.48E-05 | <i>FOXAI, KDM5B, CDKN1A, CEBPB, SRSF1, ...</i>          |
| GO:0044422                | Organelle part  | 2.45E-04 | <i>FOXAI, KDM5B, CDKN1A, CEBPB, SYNM, ...</i>           |
| <b>KEGG</b>               |   |          |   |
| hsa04115                  | p53 signaling pathway   | 2.01E-06 | <i>CDKN1A, ZMAT3, CDK4, GADD45A, MDM2, FAS, TP53</i>    |
| hsa05202                  | Transcriptional misregulation in cancer   | 4.16E-05 | <i>CDKN1A, CEBPB, MAF, SPI, MDM2, TP53, RUNX2, PBX1</i> |
| hsa04110                  | Cell cycle  | 6.97E-04 | <i>CDKN1A, CDK4, GADD45A, PLK1, MDM2, TP53</i>          |
| hsa04151                  | PI3K-Akt signaling pathway  | 0.013789 | <i>CDKN1A, CREB1, CDK4, MDM2, BRCA1, TP53, EPHA2</i>    |
| hsa05166                  | HTLV-I infection  | 0.015101 | <i>FOSL1, CDKN1A, CREB1, CDK4, TP53, ATF3</i>           |
| hsa05203                  | Viral carcinogenesis  | 0.030309 | <i>CDKN1A, CREB1, CDK4, MDM2, TP53</i>                  |
| hsa05162                  | Measles   | 0.041521 | <i>CDK4, FAS, TNFRSF10B, TP53</i>                       |
| hsa04068                  | FoxO signaling pathway  | 0.042304 | <i>CDKN1A, GADD45A, PLK1, MDM2</i>                      |

Receptor (SNARE) interactions in vesicular transport and neurotrophin signaling pathway were identified in our PPIN KEGG pathway results that could be related to side effects of DXR.

Deregulation of the cell cycle is one of the mechanisms involved in the malignant phenotype of cancer. Regulation of the cell cycle can be used as a therapeutic targeting strategy against cancer <sup>62</sup>. The chemother-

apeutic agent DXR can cause cell arrest in the G1-phase of the cell cycle<sup>63</sup>. In addition, Kim HS *et al* in 2009 reported that this drug could induce intracellular apoptotic signaling through up-regulation of Fas expression<sup>64</sup>.

Viral carcinogenesis and HTLV-1 infection were other pathways related to hubs and bottlenecks enrichments. The virus has known oncogenic potential in specific cancers, including the cervix, liver, head and neck, some lymphomas, and breast cancer<sup>65</sup>. HTLV-1 is one of the viruses that encode oncogenic protein *Tax1* Binding Protein 1 (TAX1) and help breast cancer progression<sup>66</sup>. TAX1 protein can inactivate the function of cellular TP53 and postpone the G1 cell cycle arrest required for repairing DNA in response to DNA damage<sup>67</sup>. DXR can induce apoptotic cell death in HTLV-1 infected cells<sup>68</sup>.

Our model identified that the P53 signaling pathway was a significantly enriched KEGG pathway related to hub-bottlenecks and MCODE clusters. McSweeney *et al* in 2019 reported TP53 as a critical regulator of transcriptomic changes induced by DXR<sup>69</sup>. Ru-Wei Lin *et al* in 2018 showed DXR-induced apoptosis in response to DNA damage by overexpression of TP53<sup>70</sup>. In addition, p53 interferes in cell metabolism, ferroptosis, autophagy, and generation of ROS<sup>71</sup>. These validate the predictions performed by our model and justify performing experimental examinations on its other findings.

The FoxO signaling pathway was another identified signaling predicted by the model. FoxO transcription factors are tumor suppressors that mediate redox homeostasis, proliferation, survival, and Phosphatidylinositol-4,5-Bisphosphate 3-Kinase (PI3K)<sup>72</sup>. Rosaline CY *et al*. reported that the cancer treatment with DXR increased FOXO3a activity<sup>73</sup>. During apoptosis, FOXOs are involved in expressing death receptor ligands such as Fas ligand, TNF, Bim, bNIP3, and Bcl-X<sub>L</sub><sup>74</sup>. The enhanced FOXO3a activity increased the expression of ABCB1, a plasma membrane P-glycoprotein, which functions as an efflux for various anti-cancer agents<sup>73</sup>. FOXO proteins play an essential role in glucose homeostasis by promoting gluconeogenic enzyme expression<sup>75</sup>. The dysfunction of FoxO1 pathways involves several metabolic diseases, including atherosclerosis, diabetes, non-alcoholic fatty liver disease, and obesity<sup>76</sup>. Notably, FOXO proteins are involved in physiological processes. Activation and inhibition of these proteins could have intolerable side effects.

Other signaling pathways significantly enriched in our study were SNARE interactions in vesicular transport and neurotrophin signaling pathway. SNAREs are a group of transmembrane proteins which create a bridge for interaction vesicle to its fusion partner. This vesicle trafficking is regulated by a separate process and stimulates the SNARE complex formation<sup>77</sup>. The dysfunction of membrane trafficking is associated with

cardiovascular events<sup>78</sup>. DXR disrupts the trafficking membrane by reducing *Syntaxin 17* (STX17), *Syntaxin 16* (STX16), and Synaptosome Associated Protein 29 (SNAP29) protein expression, thereby probably having side effects on the heart in this way. Besides, neurotrophins and their receptors are regulatory factors in heart and vascular development. These molecules regulate angiogenesis and vasculogenesis, controlling the survival of endothelial cells, vascular smooth muscle cells and cardiomyocytes<sup>79</sup>. Therefore, DXR may lead to cardiotoxicity through dysfunction of the neurotrophin signaling pathway with a change in expression of Glycogen Synthase Kinase 3 Beta (GSK3B), Mitogen-Activated Protein Kinase 1 (MAPK1), TP53, and Ras Homolog Family Member A (RHOA) proteins. In addition, the SNARE complex is vital in the formation of vesicle fusion, vesicle recycling and neurotransmitter release. The defects in the formation of the SNARE complex, SNARE-dependent exocytosis, and SNARE-mediated vesicle fusion are associated with neurological diseases<sup>80</sup>.

Altogether we suggest that DXR regulates repair, apoptosis, invasion and metastasis of breast cancer cells. Its side effects are probably mediated by SNARE interactions in vesicular transport and neurotrophin signaling pathway and FoxO signaling pathway through up- and down-regulated genes primarily identified in our model. Further studies *in vitro* and *in vivo* are required to validate some of our novel findings.

## Conclusion

This study applied a network-based approach (PPIN and GRN) to reveal the network hubs and bottlenecks and 3-nodes motifs consisting of TFs, miRNAs, and target genes underlying the DXR effect on breast cancer. We identified the molecular mechanisms and pathways mediating in response to DXR treatment. The hubs and bottlenecks of PPIN and GRN and PPIN MCODE clusters of differentially expressed genes in the MCF-7 cell line treated with DXR revealed that the essential biological processes and pathways are related to cell cycle, p53, viral carcinogenesis, and FoxO signaling pathway. Besides, SNARE interactions in vesicular transport and neurotrophin signaling pathway and FoxO signaling pathway were identified as pathways possibly mediating in its side effects. MCM10 and MCM3 were identified as essential DEGs mediating in response to DXR and are recommended for further investigations since their role is not studied sufficiently so far. We hope that our analysis results can understand the mechanisms involved in response to DXR and its side effects and help design further experimental investigations.

## Acknowledgement

This study is related to project NO.1398/10193 from the Student Research Committee, Shahid Beheshti University of Medical Sciences, Tehran, Iran. We also

appreciate the "Student Research Committee" and "Research and Technology Chancellor" in Shahid Beheshti University of Medical Sciences for their financial support of this study.

### Conflict of Interest

The authors declare no conflicts of interest.

### References

1. Ferlay J, Shin HR, Bray F, Forman D, Mathers C, Parkin DM. Estimates of worldwide burden of cancer in 2008: GLOBOCAN 2008. *Int J Cancer* 2010;127(12):2893-917.
2. Perou CM, Sørlie T, Eisen MB, Van De Rijn M, Jeffrey SS, Rees CA, et al. Molecular portraits of human breast tumours. *Nature* 2000;406(6797):747-52.
3. Kanavos P. The rising burden of cancer in the developing world. *Ann Oncol* 2006;17(Suppl 8):viii15-viii23.
4. Osborne CK, Zhao H, Fuqua SA. Selective estrogen receptor modulators: structure, function, and clinical use. *J Clin Oncol* 2000;18(17):3172-3186.
5. Gianni L, Norton L, Wolmark N, Suter TM, Bonadonna G, Hortobagyi GN. Role of anthracyclines in the treatment of early breast cancer. *J Clin Oncol* 2009;27(28):4798-808.
6. Rochefort H, Platet N, Hayashido Y, Derocq D, Lucas A, Cunat S, et al. Estrogen receptor mediated inhibition of cancer cell invasion and motility: an overview. *J Steroid Biochem Mol Biol* 1998;65(1-6):163-8.
7. Sisci D, Aquila S, Middea E, Gentile M, Maggiolini M, Mastroianni F, et al. Fibronectin and type IV collagen activate ER  $\alpha$  AF-1 by c-Src pathway: effect on breast cancer cell motility. *Oncogene* 2004;23(55):8920-30.
8. Chakravarty D, Nair SS, Santhamma B, Nair BC, Wang L, Bandyopadhyay A, et al. Extracellular functions of ER impact invasive migration and metastasis by breast cancer cells. *Cancer Res* 2010;70(10):4092-101.
9. Zheng S, Huang J, Zhou K, Zhang C, Xiang Q, Tan Z, et al. 17 $\beta$ -Estradiol enhances breast cancer cell motility and invasion via extra-nuclear activation of actin-binding protein ezrin. *PloS One* 2011;6(7):e22439.
10. Minotti G, Menna P, Salvatorelli E, Cairo G, Gianni L. Anthracyclines: molecular advances and pharmacologic developments in antitumor activity and cardiotoxicity. *Pharmacol Rev* 2004;56(2):185-229.
11. Arcamone F, Cassinelli G, Fantini G, Grein A, Orezzi P, Pol C, et al. Adriamycin, 14-Hydroxydaunomycin, a new antitumor antibiotic from *S. peucetius* var. *caesius*. *Biotechnol Bioeng* 2000;67(6):704-13.
12. Weiss RB. The anthracyclines: will we ever find a better doxorubicin? *Semin Oncol* 1992;19(6):670-86.
13. Doroshow JH. Role of hydrogen peroxide and hydroxyl radical formation in the killing of Ehrlich tumor cells by anti-cancer quinones. *Proc Natl Acad Sci U S A* 1986;83(12):4514-8.
14. Taylor C, Dalton W, Parrish P, Gleason M, Bellamy W, Thompson F, et al. Different mechanisms of decreased drug accumulation in doxorubicin and mitoxantrone resistant variants of the MCF7 human breast cancer cell line. *British J Cancer* 1991;63(6):923-929.
15. Yamashita H, Takahashi S, Ito Y, Yamashita T, Ando Y, Toyama T, et al. Predictors of response to exemestane as primary endocrine therapy in estrogen receptor-positive breast cancer. *Cancer Sci* 2009;100(11):2028-33.
16. McGlynn LM, Kirkegaard T, Edwards J, Tovey S, Cameron D, Twelves C, et al. Ras/Raf-1/MAPK pathway mediates response to tamoxifen but not chemotherapy in breast cancer patients. *Clin Cancer Res* 2009;15(4):1487-95.
17. Yamashita H, Nishio M, Toyama T, Sugiura H, Kondo N, Kobayashi S, et al. Low phosphorylation of estrogen receptor  $\alpha$  (ER $\alpha$ ) serine 118 and high phosphorylation of ER $\alpha$  serine 167 improve survival in ER-positive breast cancer. *Endocrine Relat Cancer* 2008;15(3):755-63.
18. Thorn CF, Oshiro C, Marsh S, Hernandez-Boussard T, McLeod H, Klein TE, et al. Doxorubicin pathways: pharmacodynamics and adverse effects. *Pharmacogenet Genomics* 2011;21:440-6.
19. Wang E, Zou J, Zaman N, Beitel LK, Trifiro M, Paliouras M. Cancer systems biology in the genome sequencing era: part 1, dissecting and modeling of tumor clones and their networks. *Semin Cancer Biol* 2013;23(4):286-92.
20. Wang E, Zou J, Zaman N, Beitel LK, Trifiro M, Paliouras M. Cancer systems biology in the genome sequencing era: part 2, evolutionary dynamics of tumor clonal networks and drug resistance. *Semin Cancer Biol* 2013;23(4):286-92.
21. Zhang N, Wang H, Fang Y, Wang J, Zheng X, Liu XS. Predicting anti-cancer drug responses using a dual-layer integrated cell line-drug network model. *PLoS Comput Biol* 2015;11(9):e1004498.
22. Magani F, Bray ER, Martinez MJ, Zhao N, Copello VA, Heidman L, et al. Identification of an oncogenic network with prognostic and therapeutic value in prostate cancer. *Mol Syst Biol* 2018;14(8):e8202.
23. Ul Ain Farooq Q, Khan FF. Construction and analysis of a comprehensive protein interaction network of HCV with its host *Homo sapiens*. *BMC Infect Dis* 2019;19(1):367.
24. Brun C, Herrmann C, Guénoche A. Clustering proteins from interaction networks for the prediction of cellular functions. *BMC Bioinformatics* 2004;5:1-11.
25. Dehghan Z, Mohammadi-Yeganeh S, Sameni M, Mirmo-talebisohi SA, Zali H, Salehi M. Repurposing new drug candidates and identifying crucial molecules underlying PCOS pathogenesis based on bioinformatics analysis. *Daru* 2021:1-14.
26. Imoto S, Tamada Y, Savoie CJ, Miyano S. Analysis of gene networks for drug target discovery and validation. *Methods Mol Biol* 2007;360:33-56.
27. Siam MKS, Shohan MUS, Syed EU. Combinatorial analysis of gene regulatory network reveals the causal genetic basis of breast cancer and gene-specific personalized drug treatments. *bioRxiv* 2020.

28. Zheng R, Wang Y, Lyu Z-I, Armaou A: Gene Regulatory Network Construction and Key Gene Recognition of Diabetic Nephropathy. In 2019 IEEE 7th International Conference on Bioinformatics and Computational Biology (ICBCB). IEEE; 2019: 1-6.
29. Aloraini A, ElSawy KM. Potential breast anti-cancer drug targets revealed by differential gene regulatory network analysis and molecular docking: Neoadjuvant docetaxel drug as a case study. *Cancer Inform* 2018;17: 1176935118755354.
30. Petrovic M, Simillion C, Kruzliak P, Sabo J, Heller M. Doxorubicin affects expression of proteins of neuronal pathways in MCF-7 breast cancer cells. *Cancer Genomics-Proteomics* 2015;12(6):347-58.
31. Chen ST, Pan TL, Tsai YC, Huang CM. Proteomics reveals protein profile changes in Doxorubicin-treated MCF-7 human breast cancer cells. *Cancer Lett* 2002;181(1):95-107.
32. Kestler HA, Müller A, Gress TM, Buchholz M. Generalized Venn diagrams: a new method of visualizing complex genetic set relations. *Bioinformatics* 2005;21(8):1592-5.
33. Szklarczyk D, Morris JH, Cook H, Kuhn M, Wyder S, Simonovic M, et al. The STRING database in 2017: quality-controlled protein-protein association networks, made broadly accessible. *Nucleic Acids Res* 2017;45(D1):D362-D368.
34. Martin A, Ochagavia ME, Rabasa LC, Miranda J, Fernandez-de-Cossio J, Bringas R. BisoGenet: a new tool for gene network building, visualization and analysis. *BMC Bioinformatics* 2010;11:91.
35. Shannon P, Markiel A, Ozier O, Baliga NS, Wang JT, Ramage D, et al. Cytoscape: a software environment for integrated models of biomolecular interaction networks. *Genome Res* 2003;13(11):2498-504.
36. Kim EY, Ashlock D, Yoon SH. Identification of critical connectors in the directed reaction-centric graphs of microbial metabolic networks. *BMC Bioinformatics* 2019;20(1):328.
37. Karbalaee R, Piran M, Rezaei-Tavirani M, Asadzadeh-Aghdaei H, Heidari MH. A systems biology analysis protein-protein interaction of NASH and IBD based on comprehensive gene information. *Gastroenterol Hepatol* 2017;10(3):194-201.
38. Kargar M, An A: The effect of sequence complexity on the construction of protein-protein interaction networks. In International Conference on Brain Informatics. Springer; 2010: 308-319.
39. Bader GD, Hogue CW. An automated method for finding molecular complexes in large protein interaction networks. *BMC Bioinformatics* 2003;4:2.
40. Huang DW, Sherman BT, Lempicki RA. Systematic and integrative analysis of large gene lists using DAVID bioinformatics resources. *Nat Protoc* 2009;4(1):44-57.
41. Szklarczyk D, Gable AL, Lyon D, Junge A, Wyder S, Huerta-Cepas J, et al. STRING v11: protein-protein association networks with increased coverage, supporting functional discovery in genome-wide experimental datasets. *Nucleic Acids Res* 2019;47(D1):D607-D613.
42. Xiao F, Zuo Z, Cai G, Kang S, Gao X, Li T. miRecords: an integrated resource for microRNA-target interactions. *Nucleic Acids Res* 2009;37(Database issue):D105-D110.
43. Hsu SD, Lin FM, Wu WY, Liang C, Huang WC, Chan WL, et al. miRTarBase: a database curates experimentally validated microRNA-target interactions. *Nucleic Acids Res* 2011;39(Database issue):D163-D169.
44. Wingender E, Dietze P, Karas H, Knüppel R. TRANSFAC: a database on transcription factors and their DNA binding sites. *Nucleic Acids Res* 1996;24(1):238-41.
45. Han H, Cho JW, Lee S, Yun A, Kim H, Bae D, et al. TRRUST v2: an expanded reference database of human and mouse transcriptional regulatory interactions. *Nucleic Acids Res* 2018;46(D1):D380-D386.
46. Tong Z, Cui Q, Wang J, Zhou Y. TransmiR v2. 0: an updated transcription factor-microRNA regulation database. *Nucleic Acids Res* 2019;47(D1):D253-D258.
47. Ahnert SE, Fink TM. Form and function in gene regulatory networks: the structure of network motifs determines fundamental properties of their dynamical state space. *J R Soc Interface* 2016;13(120):20160179.
48. Defoort J, Van de Peer Y, Vermeirssen V. Function, dynamics and evolution of network motif modules in integrated gene regulatory networks of worm and plant. *Nucleic Acids Res* 2018;46(13):6480-503.
49. Wernicke S, Rasche F. FANMOD: a tool for fast network motif detection. *Bioinformatics* 2006;22(9):1152-3.
50. Harris JR, Lippman ME, Veronesi U, Willett W. Breast cancer. *N Engl J Med* 1992;327(5):319-28.
51. Barrett-Lee P, Dixon J, Farrell C, Jones A, Leonard R, Murray N, et al. Expert opinion on the use of anthracyclines in patients with advanced breast cancer at cardiac risk. *Ann Oncol* 2009;20(5):816-27.
52. Khan NM, Diaz-Hernandez ME, Presciutti SM, Drissi H. Network analysis identifies gene regulatory network indicating the role of RUNX1 in human intervertebral disc degeneration. *Genes (Basel)* 2020;11(7):771.
53. Roy S, Raj M, Ghosh P, Das SK. Role of motifs in topological robustness of gene regulatory networks. In 2017 IEEE International Conference on Communications (ICC). IEEE; 2017: 1-6.
54. Oren M. Regulation of the p53 tumor suppressor protein. *J Biol Chem* 1999;274(51):36031-4.
55. Cortez D, Glick G, Elledge SJ. Minichromosome maintenance proteins are direct targets of the ATM and ATR checkpoint kinases. *Proc Natl Acad Sci USA* 2004;101(27):10078-83.
56. Kwok HF, Zhang SD, McCrudden CM, Yuen HF, Ting KP, Wen Q, et al. Prognostic significance of minichromosome maintenance proteins in breast cancer. *Am J Cancer Res* 2014;5(1):52-71.
57. Thu YM, Bielinsky AK. MCM10: One tool for all—Integrity, maintenance and damage control. *Seminars in Cell Developmental Biology* 2014;30:121-30.
58. Alcivar AL, Ma J, Xia B. BRCA2 interacts with an essential replication factor, MCM10. *Cancer Res* 2013; 73(8\_Supplement):1779.



59. Yang WD, Wang L. MCM10 facilitates the invaded/migrated potentials of breast cancer cells via Wnt/ $\beta$ -catenin signaling and is positively interlinked with poor prognosis in breast carcinoma. *J Biochem Mol Toxicol* 2019 Jul;33(7):e22330.
60. Ha SA, Shin SM, Namkoong H, Lee H, Cho GW, Hur SY, et al. Cancer-associated expression of minichromosome maintenance 3 gene in several human cancers and its involvement in tumorigenesis. *Clin Cancer Res* 2004;10(24):8386-95.
61. Zhou H, Xiong Y, Zhang G, Liu Z, Li L, Hou S, et al. Elevated expression of minichromosome maintenance 3 indicates poor outcomes and promotes G1/S cell cycle progression, proliferation, migration and invasion in colorectal cancer. *Biosci Rep* 2020;40(7):BSR20201503.
62. Thu K, Soria-Bretones I, Mak T, Cescon D. Targeting the cell cycle in breast cancer: towards the next phase. *Cell Cycle* 2018;17(15):1871-85.
63. Meiyanto E, Fitriyani A, Hermawan A, Junedi S, Susidarti RA. The improvement of doxorubicin activity on breast cancer cell lines by tangeretin through cell cycle modulation. *Oriental Pharmacy and Experimental Medicine* 2011;11:183-190.
64. Kim HS, Lee YS, Kim DK. Doxorubicin exerts cytotoxic effects through cell cycle arrest and Fas-mediated cell death. *Pharmacology* 2009;84(5):300-9.
65. Lawson JS, Heng B. Viruses and breast cancer. *Cancers* 2010;2(2):752-72.
66. Hirata M, Shinden Y, Nagata A, Nomoto Y, Saho H, Nakajo A, et al. Clinical features of breast cancer patients with human T-cell lymphotropic virus type-1 infection. *Asian Pacific journal of cancer prevention: Asian Pac J Cancer Prev* 2019;20(6):1909-12.
67. Pise-Masison CA, Choi KS, Radonovich M, Dittmer J, Kim SJ, Brady JN. Inhibition of p53 transactivation function by the human T-cell lymphotropic virus type 1 Tax protein. *J Virol* 1998;72(2):1165-70.
68. Mühleisen A, Giaisi M, Köhler R, Krammer P, Li-Weber M. Tax contributes apoptosis resistance to HTLV-1-infected T cells via suppression of Bid and Bim expression. *Cell Death Dis* 2014;5(12):e1575.
69. McSweeney KM, Bozza WP, Alterovitz W-L, Zhang B. Transcriptomic profiling reveals p53 as a key regulator of doxorubicin-induced cardiotoxicity. *Cell Death Discov* 2019;5:1-102.
70. Lin RW, Ho CJ, Chen HW, Pao YH, Chen LE, Yang MC, et al. P53 enhances apoptosis induced by Doxorubicin only under conditions of severe DNA damage. *Cell Cycle* 2018;17(17):2175-86.
71. Borrero LJH, El-Deiry WS. Tumor suppressor p53: Biology, signaling pathways, and therapeutic targeting. *Biochim Biophys Acta Rev Cancer* 2021;1876(1):188556.
72. Hornsveld M, Smits LM, Meerlo M, Van Amersfoort M, Koerkamp MJG, van Leenen D, et al. FOXO transcription factors both suppress and support breast cancer progression. *Cancer Res* 2018;78(9):2356-69.
73. Hui RC, Francis RE, Guest SK, Costa JR, Gomes AR, Myatt SS, et al. Doxorubicin activates FOXO3a to induce the expression of multidrug resistance gene ABCB1 (MDR1) in K562 leukemic cells. *Mol Cancer Ther* 2008 Mar;7(3):670-8.
74. Farhan M, Wang H, Gaur U, Little PJ, Xu J, Zheng W. FOXO signaling pathways as therapeutic targets in cancer. *Int J Biol Sci* 2017 Jul 6;13(7):815-27.
75. Gross D, Van den Heuvel A, Birnbaum M. The role of FoxO in the regulation of metabolism. *Oncogene* 2008;27(16):2320-36.
76. Peng S, Li W, Hou N, Huang N. A review of FoxO1-regulated metabolic diseases and related drug discoveries. *Cells* 2020;9(1):184.
77. Lowenstein CJ. Nitric oxide regulation of protein trafficking in the cardiovascular system. *Cardiovasc Res* 2007;75(2):240-6.
78. Enrich C, Rentero C, Hierro A, Grewal T. Role of cholesterol in SNARE-mediated trafficking on intracellular membranes. *J Cell Sci* 2015;128(6):1071-81.
79. Caporali A, Emanuelli C. Cardiovascular actions of neurotrophins. *Physiol Rev* 2009;89(1):279-308.
80. Margiotta A. Role of SNAREs in neurodegenerative diseases. *Cells* 2021;10(5):991.

## Regulatory Motifs in Doxorubicin Effects

### Supplementary

Supplementary Table S1. Up/Down-regulated proteins are represented below

| Up regulated | Down regulated | Up regulated | Down regulated | Up regulated | Down regulated |
|--------------|----------------|--------------|----------------|--------------|----------------|
| BTG2         | ESPL1          | CAT          | DLGAP5         |              | ZFR            |
| GDF15        | E2F8           | TP53B3       | RAD51AP1       |              | PBRM1          |
| WISP2        | ORC3           | CCS          | MKI67          |              | NKRF           |
| HIC2         | TPX2           | PML          | DTL            |              | PRDM15         |
| TIGAR        | GPSM2          | PRKD1        | PAICS          |              | ZFP2           |
| EPHA2        | CCNB1          | PXN          | MPHOSPH9       |              | TTC5           |
| ATF3         | BRCA1          | HBA2         | MCM6           |              | C17orf49       |
| FAS          | BIRC5          | LIG1         | CENPI          |              | ZBTB9          |
| TAP1         | PLK1           | CDK1         | CCNF           |              | HIST2H2AB      |
| XPC          | ST8SIA4        | PRKAA1       | SLC25A12       |              | YY2            |
| NADSYN1      | TUBB           | ASNS         | KIF20A         |              | HIST2H3D       |
| KRT15        | CHEK1          | CDH1         | TTK            |              | RFX8           |
| MOSPD1       | MUC1           | CDK4         | CDKN3          |              | CREB1          |
| STOM         | KIF11          | CDKN1A       | NCAPG          |              | PNKP           |
| YPEL5        | SKP2           | MPST         | CENPF          |              | PURB           |
| AVP1         | ORC1           | SCFD1        | AKAP8          |              | NABP2          |
| DPYSL4       | CDC6           | HMGCL        | PES1           |              | TAF2           |
| GM2A         | ZWILCH         | SMARCA5      | H2AF           |              | TAF7           |
| DUSP1        | DBF4           | FOXD4L1      | MKI67IP        |              | MTA2           |
| WSB1         | KIF14          | MSH2         | CSNK1A1        |              | HOXC11         |
| PHYH         | MAD2L1         | SRSF1        | PPP1CC         |              | HOXD10         |
| ZMAT3        | POLA1          | GNA13        | BUB3           |              | ALX1           |
| LIMK2        | AURKB          | PITPNB       | NDE1           |              | MYBBP1A        |
| TP53B3       | MCM3           | TANC2        | ERCC6L         |              | VSX1           |
| AK1          | TIPIN          | EPN1         | SPC24          |              | POLE4          |
| PSG9         | C17orf75       | MBD3         | NUP43          |              | STX16          |
| EPPK1        | KIF4A          | RIC8A        | LIG3           |              | SNAP29         |
| TMEM158      | BAR1           | GRSF1        | NSMCE2         |              | STX17          |
| GADD45A      | MCM10          | AMBRA1       | PARP1          |              | TLK1           |
| MDM2         | FBXO5          | PPP1R13L     | BCL3           |              | HIRIP3         |
| TRAF4        | MELK           | MLL          | CCNT1          |              | ASF1B          |
| CSAD         | CDC20          | POU4F3       | DNA2           |              | ACTL6A         |
| SLC6A8       | GART           | PRKRA        | ENO1           |              | SUPT4H1        |
| TNFRSF10B    | NDC80          | RUNX2        | GATA3          |              | LEO1           |
| ARFGAP3      | CCNA2          | DLG1         | GTF2A1         |              | MRGBP          |
| MAFB         | GTSE1          | ALB          | H1FO           |              | UTP3           |
| CABYR        | BUB1           | GSTK1        | HIST1H1E       |              | SRPK1          |
| CDKN1A       | PBK            | PRDX4        | HIST1H1B       |              | BRD8           |
| MORC4        | DEPDC1         | SNAPIN       | HMGN1          |              | PRMT5          |
| MAF          | NCAPH          | DTNBP1       | AGFG1          |              | PYGO2          |
| FDXR         | MDC1           | SLC6A17      | MCM3           |              | GPI            |
| PIDD1        | PFAS           | TRIM37       | NFYB           |              | C3             |
| GPR87        | HNRNP          | CHP1         | PBX1           |              | MTPN           |
| ACTA2        | CENPE          | PYCARD       | POLR2C         |              | OGDH           |
| ANXA4        | ASPM           | NR3C2        | MAPK1          |              | HPRT1          |
| SYNM         | UBE2S          | NFYC         | RFC2           |              | MYCBP2         |
| CYFIP2       | LMNB1          | ZNF24        | RPL6           |              | MAP2           |
| FOSL1        | PRIM1          | MTA1         | SMARCA1        |              | ANXA1          |
| PDE4A        | CDCA3          | ZGPAT        | SMARCC1        |              | RYK            |
| GLS2         | ATAD2          | ARX          | SP100          |              | UACA           |
| SAT1         | BRIP1          | FOSL2        | SURF6          |              | CD276          |
| GABPA        | STIL           | NUP93        | BRPF1          |              | CTNNA2         |
| TP53         | UBE2C          | NUP153       | DEK            |              | MYO1D          |
| CEBPB        | CCNB2          | NUP107       | KDM5D          |              | DDN            |
| FOXA1        | MCM7           | GSK3A        | ARID1A         |              | LIMS1          |
| SP1          | PRC1           | GSK3B        | HIST2H2AC      |              | RHOA           |
| ANK3         | CDT1           | PREP         | NCOR2          |              | LTBP2          |
| GOLGA4       | CDC45          | CTSA         | BCLAF1         |              | PPM1A          |
| ARFRP1       | GEMIN2         | SCPEP1       | TOX4           |              | PPP1CB         |
| MACF1        | SPC25          | ARHGEF2      | SRA1           |              | UBA52          |
| NQO1         | WDHD1          |              | HUWE1          |              | SNX6           |
| NUDT1        | MCM2           |              | PQBP1          |              | ANKRD17        |
| NDUFS8       | DUT            |              | SRRM1          |              |                |
| RRM2B        | KIF18A         |              | KDM5B          |              |                |
| NAPRT1       | KIF15          |              | AKAP8L         |              |                |
| SRXN1        | MSH2           |              | NUSAP1         |              |                |

Supplementary Table S2. Hubs and bottlenecks (top 10%) related to PPI network obtained by Cytoscape software

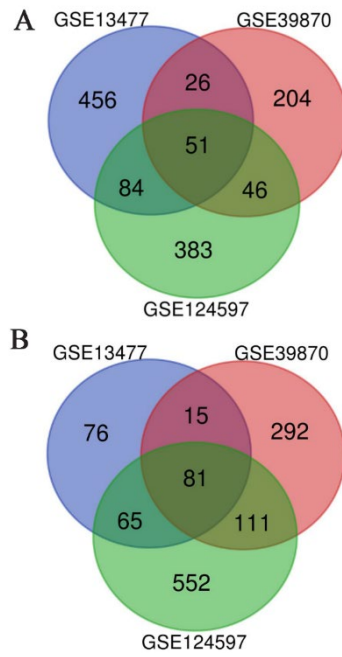
| 10% degree and betweenness centrality |
|---------------------------------------|
| CDK1                                  |
| TP53                                  |
| CCNB1                                 |
| CCNA2                                 |
| CDC20                                 |
| BUB1                                  |
| PLK1                                  |
| NDC80                                 |
| CCNB2                                 |
| CDC6                                  |
| AURKB                                 |
| KIF11                                 |
| MAD2L1                                |
| UBA52                                 |
| MCM2                                  |
| MCM10                                 |
| CHEK1                                 |
| CDC45                                 |
| BIRC5                                 |
| UBE2C                                 |
| NCAPG                                 |
| TTK                                   |
| CENPF                                 |
| MCM3                                  |
| PBK                                   |
| TPX2                                  |
| STX16                                 |
| SNAP29                                |
| GOLGA4                                |
| ARFRP1                                |
| SCFD1                                 |
| MAPK1                                 |
| STX17                                 |
| HIST2H2AC                             |
| RHOA                                  |
| BRCA1                                 |
| GSK3B                                 |
| POLR2C                                |
| TUBB                                  |
| CDH1                                  |

## Regulatory Motifs in Doxorubicin Effects

Supplementary Table S3. Each column represents proteins available in one MCODE cluster

| Subnetwork 1 | Subnetwork 2 | Subnetwork 3 |
|--------------|--------------|--------------|
| CDC45        | ASF1B        | GTF2A1       |
| TTK          | PRIM1        | NAPRT        |
| MELK         | PPP1CC       | GM2A         |
| BUB1         | MCM3         | C3           |
| CCNB2        | ORC1         | PBRM1        |
| DLGAP5       | MCM7         | MAPK1        |
| KIF15        | ZWILCH       | TUBB         |
| KIF20A       | NDE1         | PARP1        |
| CDKN3        | ERCC6L       | HIST2H2AC    |
| CDCA3        | NUP43        | ARID1A       |
| KIF14        | CDT1         | SMARCC1      |
| BIRC5        | SPC24        | BARD1        |
| MKI67        | CENPI        | ACTL6A       |
| KIF11        | NUP107       | LIG3         |
| DTL          | BUB3         | PRMT5        |
| CDK1         |              | MDC1         |
| KIF4A        |              | CTSA         |
| NDC80        |              | PYCARD       |
| CENPE        |              |              |
| CDC6         |              |              |
| CENPF        |              |              |
| CDC20        |              |              |
| GTSE1        |              |              |
| PRC1         |              |              |
| CCNA2        |              |              |
| UBE2C        |              |              |
| ASPM         |              |              |
| PLK1         |              |              |
| CCNB1        |              |              |
| MCM2         |              |              |
| MCM6         |              |              |
| NCAPG        |              |              |
| CHEK1        |              |              |
| MAD2L1       |              |              |
| RAD51AP1     |              |              |
| PBK          |              |              |
| AURKB        |              |              |
| NCAPH        |              |              |
| KIF18A       |              |              |
| TPX2         |              |              |
| ESPL1        |              |              |
| SPC25        |              |              |
| NUSAP1       |              |              |
| MCM10        |              |              |
| DEPDC1       |              |              |





Supplementary Figure S1. Venn diagram for DEGs of GEO datasets (GSE124597, GSE39870, and GSE13477) related to MCF-7 cell line treated with doxorubicin. A) Venn diagram related to up-regulated genes B) Venn diagram related to down-regulated genes.